metals

MDPI

Article

# Ti/Al Multi-Layered Sheets: Accumulative Roll Bonding (Part A)

**Jan Romberg [1,2], Jens Freudenberger [1,2,3,*], Hansjörg Bauder [4], Georg Plattner [4], Hans Krug [4], Frank Holländer [5], Juliane Scharnweber [6], Andy Eschke [6], Uta Kühn [1], Hansjörg Klauß[1], Carl-Georg Oertel [6], Werner Skrotzki [6], Jürgen Eckert [7,8] and Ludwig Schultz [1,2]**

1 Leibniz Institut für Festkörper- und Werkstoffforschung Dresden (IFW Dresden), Helmholtzstr. 20, Dresden D-01069, Germany; janromberg@yahoo.de (J.R.); u.kuehn@ifw-dresden.de (U.K.); h.j.klauss@ifw-dresden.de (H.K.); l.schultz@ifw-dresden.de (L.S.)
2 Institut für Werkstoffwissenschaft, Technische Universität Dresden, Dresden D-01062, Germany
3 Institut für Werkstoffwissenschaft, Technische Universität Bergakademie Freiberg, Gustav-Zeuner-Str. 5, Freiberg D-09599, Germany
4 Carl Wezel KG, Industriestr. 95, Mühlacker D-75417, Germany; carl_wezel_kg@t-online.de (H.B.); carl_wezel_kg@t-online.de (G.P.); hk.krug@gmx.net (H.K.)
5 Lehrstuhl Metallkunde und Werkstofftechnik, Brandenburgische Technische Universität Cottbus, Konrad-Wachsmann-Allee 17, Cottbus D-03046, Germany; hollaend@tu-cottbus.de
6 Institut für Strukturphysik, Technische Universität Dresden, Dresden D-01062, Germany; juliane.scharnweber@tu-dresden.de (J.S.); andy.eschke@gmx.de (A.E.); oertel@physik.tu-dresden.de (C.-G.O.); werner.skrotzki@physik.tu-dresden.de (W.S.)
7 Erich Schmid Institut für Materialwissenschaft, Österreichische Akademie der Wissenschaft, Jahnstraße 12, Leoben A-8700, Austria; juergen.eckert@unileoben.ac.at
8 Department Materialphysik, Montanuniversität Leoben, Jahnstraße 12, Leoben A-8700, Austria
* Correspondence: j.freudenberger@ifw-dresden.de; Tel.: +49-351-4659-550; Fax: +49-351-4659-541

Academic Editor: Hugo F. Lopez
Received: 26 November 2015; Accepted: 25 January 2016; Published: 2 February 2016

**Abstract:** Co-deformation of Al and Ti by accumulative roll bonding (ARB) with intermediate heat treatments is utilized to prepare multi-layered Ti/Al sheets. These sheets show a high specific strength due to the activation of various hardening mechanisms imposed during deformation, such as: hardening by grain refinement, work hardening and phase boundary hardening. The latter is even enhanced by the confinement of the layers during deformation. The evolution of the microstructure with a special focus on grain refinement and structural integrity is traced, and the correlation to the mechanical properties is shown.

**Keywords:** accumulative roll bonding; Ti/Al multi-layered composites; grain refinement; microstructure; mechanical properties

## 1. Introduction

Light weight materials are in the focus of the development of novel structural materials, as they bear the potential to reduce the energy consumption in mobile applications while retaining the functionality. There are numerous approaches to obtain materials with a high specific strength. On the one hand, novel steels are developed to complement the most dominant class of structural materials and to extend their field of usability to light weight applications [1–3]. On the other hand, the "classic" light weight materials for structural applications with densities below 4.5 g/cm$^3$, such as Ti, Al, Mg and their alloys, are optimized with respect to strength. For this purpose, various means are utilized, including alloy design and the development of novel processing techniques [4–6]. The latter also

involves non-common deformation techniques, such as the application of severe plastic deformation (SPD) [7–11] or co-deformation of at least two different materials [12–16].

Co-deformation of two metallic materials, such as Al and Ti, bears the potential to gain improved material properties regarding strength and formability. Both material properties are strongly linked to the microstructure. Their evolution including the formation of texture in these materials represents the key aspect in developing materials with superior properties. In recent years, it has been shown that cold working to large plastic strains can impose ultra-fine grained microstructures [17–19] or even microstructures with features being in the nanometer range [20–22]. The small grain sizes, fine dislocation networks and/or small precipitates cause a significant contribution to the mechanical strength according to Hall–Petch-type, work and precipitation hardening, respectively [8,23–25]. When applied in combination, these hardening mechanisms may even have a synergetic strength effect. When co-deformation is applied repetitively, as is the case for accumulative roll bonding (ARB) [26–28] and for accumulative swaging and bundling (ASB) [16,29–33], the density of phase boundaries increases with applied bonding or bundling cycles, respectively. The increasing number of phase boundaries is beneficial for two reasons. First, the phase boundary itself represents a barrier for dislocation movement [34]. Secondly, these phase boundaries limit possible grain growth. After deformation to very large plastic strains, the multi-phased materials have a mean phase boundary distance in the the sub-micrometer-range. These materials also show considerable strength at elevated temperatures when grain growth occurs in at least one phase, as grain growth is limited to the distance of the phase boundaries. Summarizing, high densities of grain and phase boundaries significantly contribute to the strength of metallic composites.

Although it has already been shown that Ti/Al composite sheets can be obtained by ARB [35–40], this process remains difficult. A crucial issue is to retain individual continuous layers within the composite during accumulative deformation. Once the Ti layers are strain hardened beyond a certain limit, their formability is negligible when compared to the Al sheets. Consequently, necking of the Ti layers is observed, and the stretched Ti pieces remain rather stable in size within the continuously-deforming Al matrix [36,41–43].

In contrast to this, the individual Ti and Al layers remain stable when an intermediate heat treatment (IHT) is applied between the rolling cycles. After eight ARB + IHT cycles, a fine multi-layered composite sheet is obtained. With respect to grain refinement, IHT is counter-productive, as it may cause recovery, recrystallization and grain growth. Consequently, a highly strengthened light weight material cannot be achieved with this procedure. In addition, it is necessary to emphasize that the individual layers become wavy with increasing deformation strain, *i.e.*, the number of ARB cycles, which has been considered as a consequence of the evolution of the texture within the layers [44,45].

To avoid necking, a high work hardening rate and a low strength level are necessary. During the first ARB cycle, these conditions are met, but already for the second cycle, the work hardening ability of Ti is already saturated and, thus, may be responsible for the necking of the Ti layers. An annealing treatment at 723 K for 90 min under vacuum conditions between each ARB cycle lowers the strength, and the strain hardening ability is restored. Optimum strain hardening conditions would possibly be restored above the transus temperature of Ti. However, this is not possible to apply to the composite, as this temperature is above the melting temperature of Al.

At elevated temperatures, successful roll bonding of Al can be achieved using a lower thickness reduction. It can be expected that this would result in reduced necking of the Ti layers. However, the reduction of strength with rising temperature is less pronounced in Ti than in Al. Alternatively, the arrangement of rolls and the geometry of the rolling gap can be altered. In contrast to a four high rolling mill, which is symmetric with respect to the sheet plane, trio rolling with different sizes of the upper and lower rolls is asymmetric. Even in the case when the excenter velocities of the upper and lower rollers are identical, the difference in diameter causes shearing in the deformation zone and, thus, eases bonding and reduces necking. This second possibility of controlling the homogeneity

of the layers' appearance is addressed in Part B of the present study (Ti/Al Multi-Layered Sheets: Differential Speed Rolling). This article addresses the influence of ARB on the microstructure, as well as on the appearance and faults of the individual layers; four different solutions to receive finely-layered Ti/Al composite sheets by ARB are discussed: the effect of intermediate heat treatments, temperature, strain rate and that of the confinement in the deformation zone.

## 2. Experimental Section

ARB was performed on a stack of five layers composed of pure Ti (99.995%) and the aluminum alloy AA5049 (Al, 2% Mg and 0.8% Mn; in the following referred to as Al) sheets with a thickness of 1 mm each. This stack (Al-Ti-Al-Ti-Al) with an initial height of 5 mm was reduced by 50% in thickness within one single rolling pass. Subsequently, the sheets were cut in length into two pieces, wire-brushed after cleaning with ethanol, stacked and further roll bonded. The ARB cycles were repeated up to eight times. To investigate the effect of rolling speed on the formation of the microstructure, two series of sheets have been produced with different rolling speeds. Some sheets have been intermediately heat treated at 723 K for 90 min under vacuum conditions ($p \leq 10^{-5}$ mbar). The deformation rate was determined from the rolling speed assuming constant rolling speed and neglecting shear deformation.

The influence of temperature on ARB was studied for the second and fourth ARB cycle. The initial bonding has always been performed at room temperature (RT). For ARB at elevated temperature, the rolls were heated up to 573 K. The temperature at which the samples have been heated before rolling varied from RT to 573 K.

The microstructure has been observed by scanning electron microscopy (SEM, Zeiss Microscopy, Jena, Germany) and electron backscatter diffraction (EBSD, Oxford Instruments, Abingdon, UK) after metallographic preparation, described in detail elsewhere [43]. EBSD measurements were done in the upper third of the single material sheets and the 160-layer composite sheets. In the 5-layer sheets, EBSD maps were measured within the top layer (aluminum) and the second-top layer (titanium). The step size for EBSD mapping was 200 nm and 40 nm for Al and Ti, respectively. Areas separated by grain boundaries with misorientations of more than 15° are considered as grains. The grain size is given as the median number-weighted and the median area-weighted grain size. The first metric captures predominantly small grains, the second measures particularly large grains, especially in wide spread grain size distributions. Consequently, two values are obtained on the same data, representing lower and upper bounds for the grain size. The latter method implies that 50% of the cross-sectional area is covered by grains with a size larger than the median value. The advantage of this procedure is that the sensitivity to detect changes in the grain size distribution is enhanced, and the effect of rolling on the microstructure can be traced more easily. EBSD also provides information about the orientation distribution in a generally small area of the sheets, *i.e.*, the local texture with a poor statistic is reflected.

Tensile tests were carried out at RT at a constant strain rate of 0.01 $s^{-1}$ utilizing an electro-mechanical Instron 8562 testing machine. The geometry of the test specimens is shown in Figure 1. The thickness of the tensile test specimens varied, as the samples were cut from the as-rolled sheets. The initial sheets had a thickness of 1 mm, and the sheets that have been subjected to ARB had a thickness of about 2.5 mm.

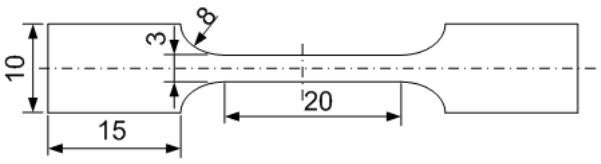


**Figure 1.** Geometry of the samples used for tensile tests. Dimensions are provided in mm.

## 3. Results and Discussion

### *3.1. Intermediate Heat Treatment*

Roll bonding of five sheets with a thickness reduction of 50% does not significantly affect the grain size. Therefore, the effect of further processing by ARB is addressed in the following. Figure 2 shows the layer and phase distribution of Ti/Al composites after different ARB cycles. It can be seen that the Ti layers (bright grey) are not continuous anymore after four or more ARB cycles at room temperature and no IHT applied. Under the mentioned conditions, Al layers remain continuous. Therefore, they are capable of the observed plasticity. Further argument for this assumption is taken from the layer thickness: Al layers are thinner than the Ti layers, although their initial thickness was the same. Furthermore, the Al flows in between the Ti flakes. Both features support the conclusion that the Ti layers are locally sheared in bands, but not continuously thinned. Indeed, the Ti flakes do not show a considerable change in their size with further deformation.

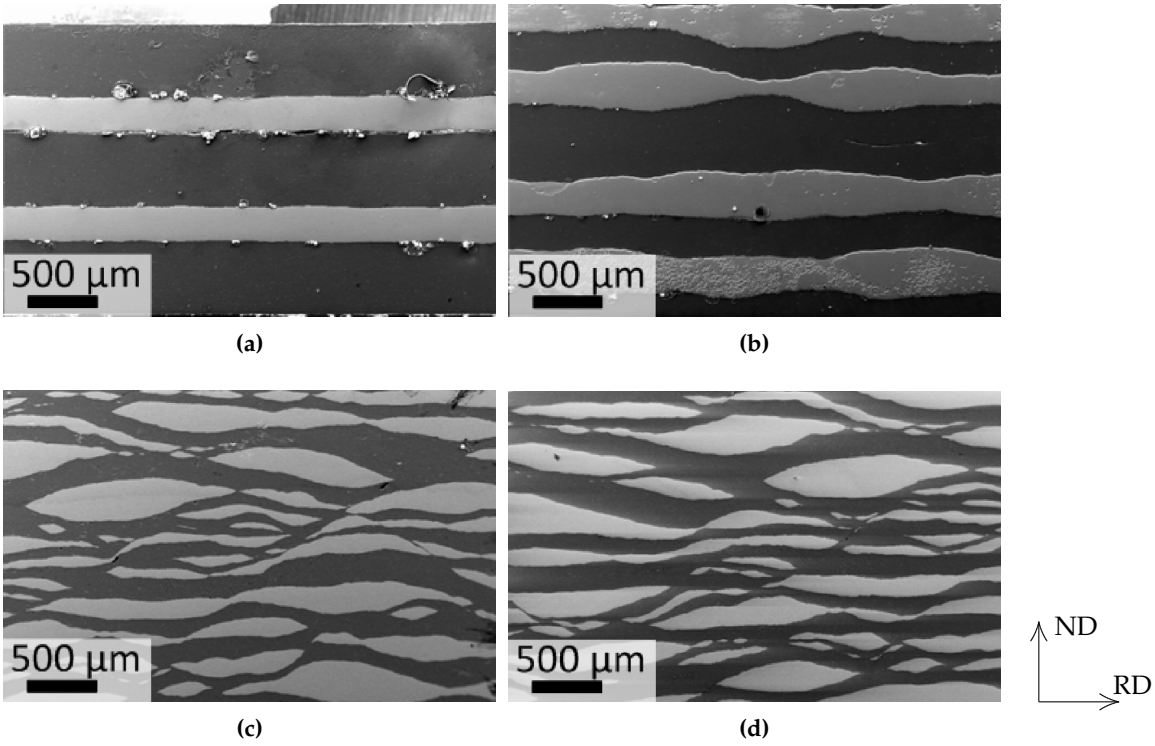


**Figure 2.** SEM micrographs showing the longitudinal cross-section of Ti/Al composite sheets after accumulatively roll bonding a five-layered composite, *i.e.*, after the first (**a**), second (**b**), fourth (**c**) and sixth (**d**) accumulative roll bonding (ARB) cycle (no intermediate heat treatment (IHT) was applied).

Nevertheless, the mechanical properties of the five-layered composite, as well as the further ARB processed composite are investigated. Figure 3 shows the evolution of the mechanical properties with respect to the number of ARB cycles.

Roll bonding of three Al and two Ti sheets to the five-layered composite (*i.e.*, the first ARB cycle) causes a remarkable decrease of the plastic strain when comparing the composite to pure Ti. This decrease is still significant, but less pronounced when comparing the composite to pure Al. This processing step on the other hand leads to an increase of yield and ultimate tensile strength by a factor of about two. Further processing by ARB does not change the mechanical properties significantly, which is mainly attributed to the discontinuous layers. The work hardening ability of Ti reaches its limit; therefore, the contribution to strain of Ti is shrinking. Furthermore, Al shows dynamic recovery

during further processing. Thus, this processing route is not promising for obtaining ultra-fine grained materials with a large number of interfaces, as at a higher number of ARB cycles, the Ti flakes produced are circumvented by Al flow, as can be seen from the similar SEM micrographs obtained on sheets being deformed with four and six ARB cycles (Figure 2c,d). In order to retain the formability of the Ti-layers within the composite, IHTs have been introduced after each roll bonding step. These IHTs were performed at 723 K for 90 min under vacuum conditions ($p \leq 10^{-5}$ mbar) and are applied to retain the formability of the composite. Furthermore, the individual Ti layers remain continuous during the ARB cycles. The corresponding layer structures are shown in Figure 4.

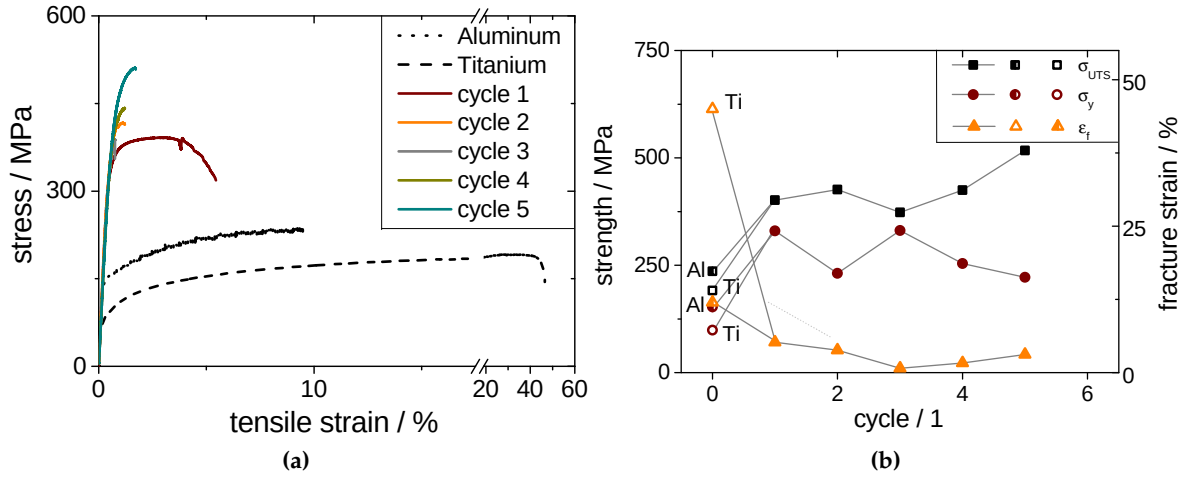


**Figure 3.** Engineering stress-strain curves of the five-layered Ti/Al composite accumulatively roll bonded with up to five cycles without intermediate heat treatments (**a**) and ultimate tensile strength ($\sigma_{UTS}$), yield strength ($\sigma_y$) and plastic strain ($\varepsilon$) of Al (half open symbols), Ti (open symbols) and the five-layered composite (filled symbols) (**b**).

Unfortunately, the IHT causes recrystallization of the Al, as well as recovery of the Ti. These processes are reflected by the grain size. Figure 5 shows the evolution of the grain size within the Ti and Al layers during processing by ARB. In order to make this evaluation comparable to others, the weighting methods described in the Experimental Section have been applied.

Without IHT, the mean grain size of both phases is lowered during ARB. This reduction is pronounced within the first to third ARB cycle. Subsequent ARB cycles lead to a steady state of the grain size in the sub-micrometer range.

The grain sizes are also determined after each ARB cycle before and after additional IHTs (pre-IHT and post-IHT). The grain size is larger in the heat-treated samples due to grain growth. Additional ARB does not reduce the grain size to the condition observed without IHTs.

Anyhow, the change in grain size due to the deformation by ARB with and without IHTs is small in the present case. Therefore, it is quite expectable that the mechanical strength of the composites remains at a comparable level. The tensile properties of the Ti/Al composites as prepared by increasing ARB cycles with intermediate heat treatments are shown in Figure 6.

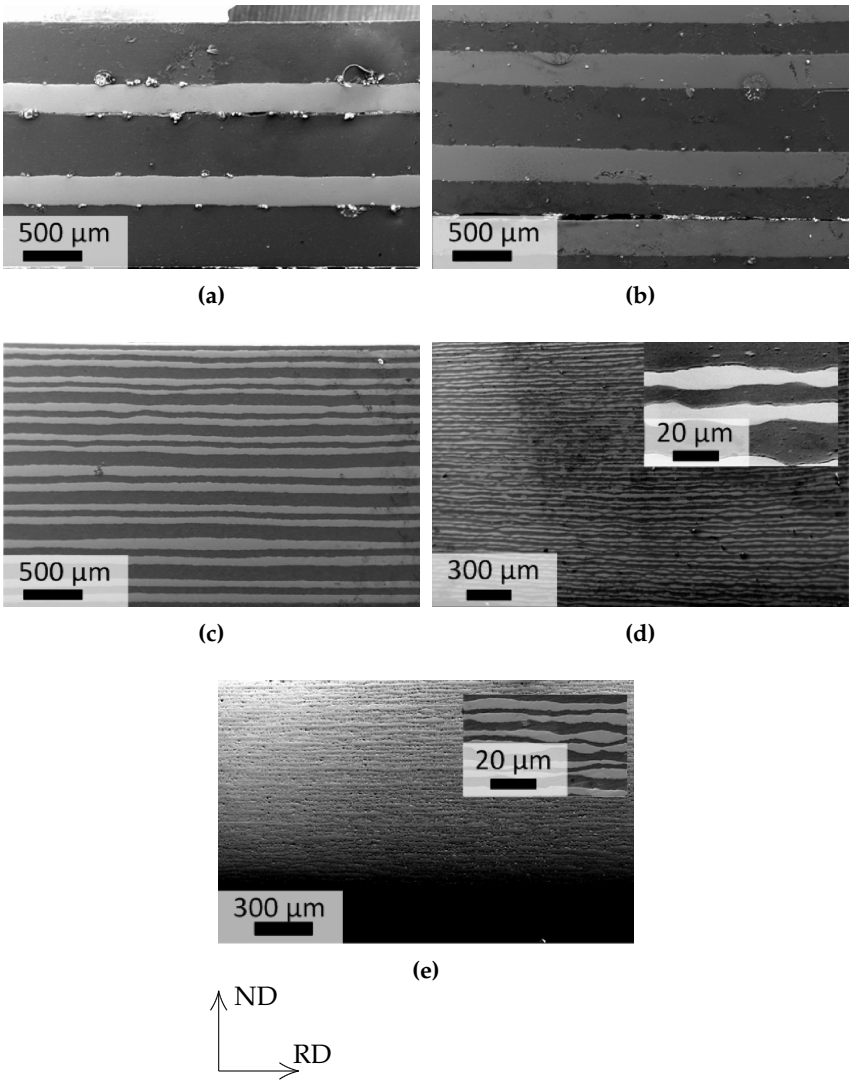


**Figure 4.** SEM micrographs showing the longitudinal cross-section of the layer structure of a Ti/Al composite sheets after accumulatively roll bonding a five-layered composite after the first (**a**), second (**b**); fourth (**c**), sixth (**d**) and eighth (**e**) ARB cycle with IHTs being applied.

The engineering stress-strain curves reveal ultimate tensile strength values ranging from 375 MPa to 406 MPa. In contrast to the common strength values of the composites, a different behavior is observed for the plastic strain. After the first ARB cycle, the stress-strain curve shows the maximum strength and an uniform elongation of about 3%. Further straining causes remarkable jumps in the stress-strain curve, which are related to the failure of the individual layers of the composite. Obviously, the bonding between these layers is not sufficient at this stage of deformation. Already after the next ARB cycle, just one single step remains visible, indicating that bonding has improved.

The reason for the disappearing of the steps in the stress-strain curve is related to the processing of the composites. In the first ARB step, the Ti and Al layers have to be roll bonded. This is the most difficult processing step of the Ti/Al composite materials. Later ARB cycles only bond outer Al layers, which is much easier. The inner Ti/Al interfaces become more perfect during each rolling cycle, and thus, their bonding strength further increases.

Considering a Ti/Al five-layered composite after the first ARB cycle: when the first layer fails, the fracture toughness of the composite has been reached, causing macroscopic fracture. With further ARB cycles, the number of layers increases. The failure of an individual layer does not cause the

shear strength to be larger than the fracture stress, and consequently, the observed plastic strain is larger. This situation, however, changes again with further deformation by ARB, as a further reinforcement caused by the improvement of the bonding strength of the interface due to further rolling is observed. As a consequence, a reduction of the plastic strain is gained. Hence, optimum plasticity is observed for the composite with stabilized interfaces and a certain, but not too small number of layers. A further enlargement of the number of individual layers would not be beneficial with respect to the plasticity at this processing step, unless the material shows a grain size in the nanometer range [7,19,46].

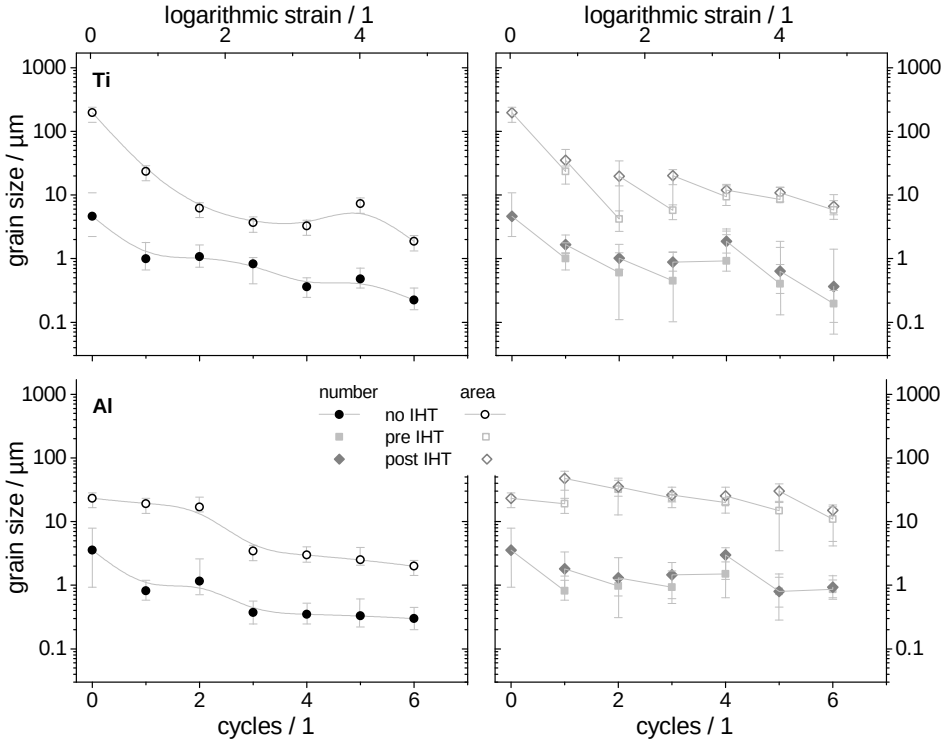


**Figure 5.** Grain size within the Ti (upper row) and Al layers (lower row) after ARB at room temperature (left), as well as with IHTs applied (right). In the latter case, the grain sizes are provided after the ARB cycles before (pre-IHT) and after IHT (post-IHT). The grain sizes were evaluated by both number and area weighting.

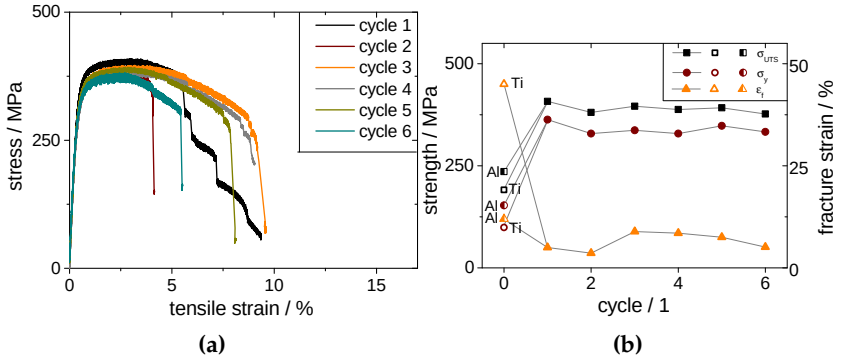


**Figure 6.** Engineering stress-strain curves of the five-layered Ti/Al composite accumulatively roll bonded with up to six cycles, including intermediate heat treatments (IHT) (**a**) and ultimate tensile strength ($\sigma_{UTS}$), yield strength ($\sigma_y$) and plastic strain ($\varepsilon$) of Al (half open symbols), Ti (open symbols) and the five-layered composite (filled symbols) (**b**).

### 3.2. Deformation Speed

ARB has also been performed at different strain rates, established by varying the rolling velocity. Here, results for strain rates of 5.3 $s^{-1}$ and 23.4 $s^{-1}$ are discussed. Figure 7 shows the corresponding layer structure obtained after four ARB cycles. It is observed that slow rolling results in enhanced necking of the Ti layers. The grains within Al and Ti are elongated in the rolling direction.

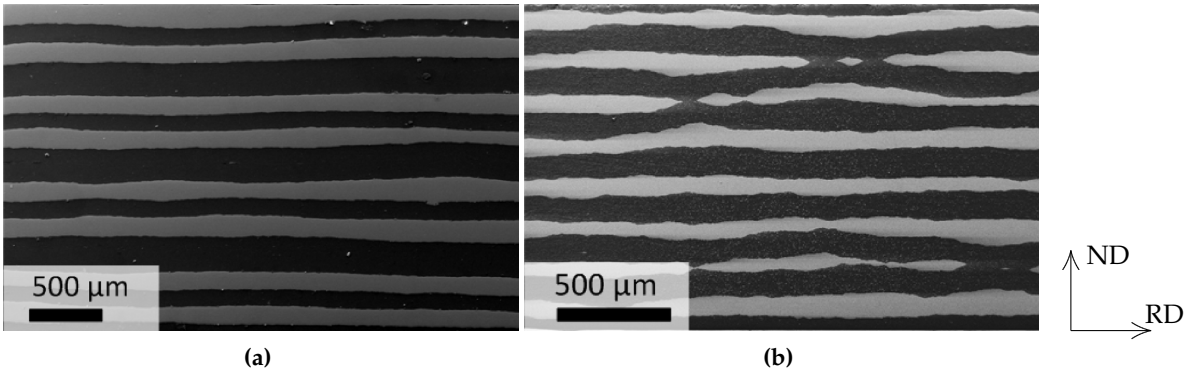


**Figure 7.** Micrographs showing the longitudinal sections of five-layered composites after four ARB cycles; rolling with a strain rate of 23.4 $s^{-1}$ (**a**) and 5.3 $s^{-1}$ (**b**).

As discussed by Emmens [47], work hardening delays or avoids necking. The effect is more pronounced if the strain rate sensitivity is high, because the necked regions deform with a higher strain rate compared to the rest of the material. Therefore, the necked material is hardened and consequently becomes less deformed. According to this observation, the strain rate sensitivity for Ti is higher for the strain rate of 23.4 $s^{-1}$ than for 5.3 $s^{-1}$. Consequently, less necking occurs for deformation at large strain rates. Combining IHT and a high strain rate enables more stable deformation conditions, yielding a laminar structure after eight ARB cycles. The microstructure of Al contains a small number of elongated grains, while the majority of the grains is equiaxed. The grain size of most grains is limited by the layer thickness. The Ti grains are smaller than the layer thickness. There is also a mixture of elongated and equiaxed grains, as shown in Figure 8.

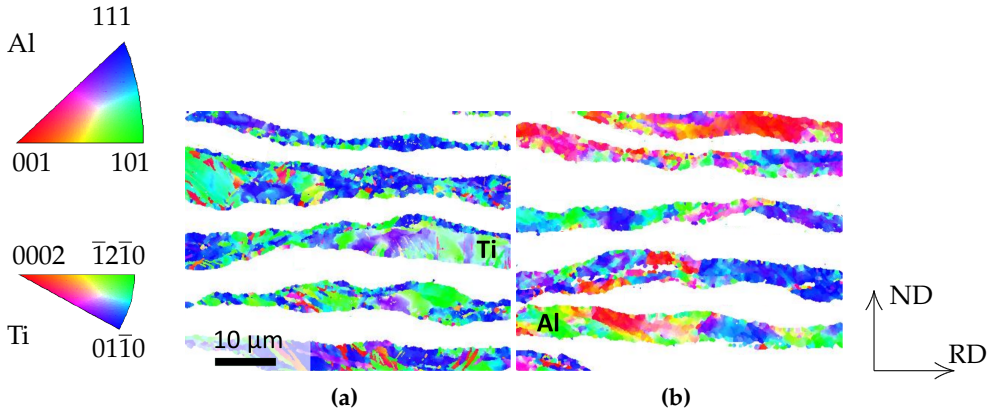


**Figure 8.** Electron backscatter diffraction (EBSD) maps of a five-layered composite sheet after eight ARB + IHT cycles. The maps are separated for Ti (**a**) and Al (**b**). The color code describes the crystal orientation in the rolling direction according to the inverse pole figure maps (shown leftmost for the cubic (Al, upper part) and hexagonal case (Ti, lower part)).

### *3.3. ARB at Elevated Temperatures*

ARB has also been performed at elevated temperatures. For this purpose, two five-layered composites that were roll bonded at RT were further rolled at higher temperatures. It turned out that this condition requires a modification of the applied strain, as thermal softening is superimposed by strain hardening. The applicability of the process is evaluated after the second ARB cycle. The corresponding results are summarized in Table 1. Micrographs of the corresponding layer structures are shown in Figure 9 for the case of successful processing.

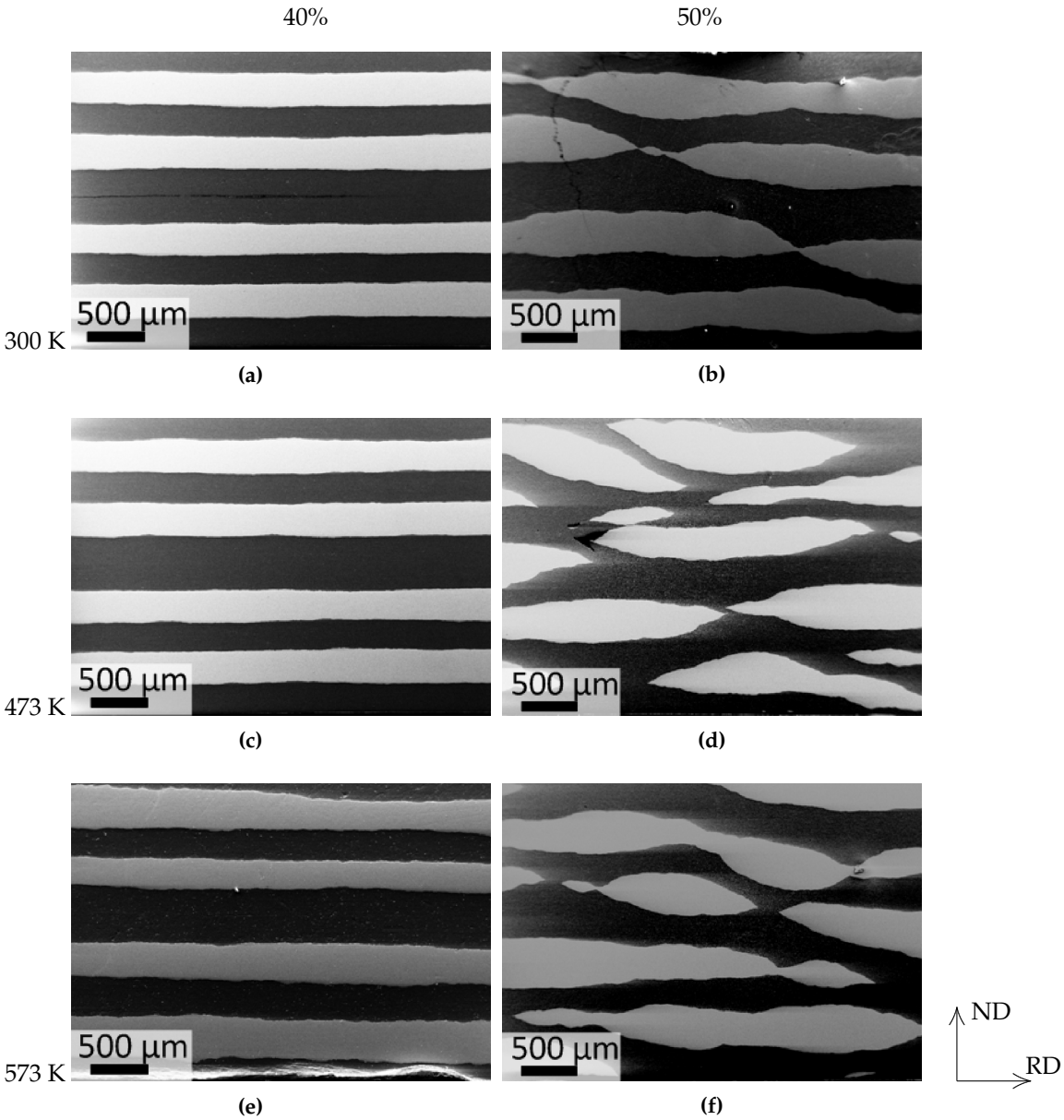


**Figure 9.** SEM micrographs showing the layer structure of a five-layered composite roll bonded with a single ARB cycle at elevated temperatures. The sheets are rolled with a 40% (**a**,**c**,**e**) or a 50% (**b**,**d**,**f**) thickness reduction during the second cycle.

**Table 1.** Overview of elevated temperature ARB.

| Temperature | Thickness Reduction | | |
|---|---|---|---|
| | **30%** | **40%** | **50%** |
| RT | no bonding | weak bonding<br>laminar layers | strong bonding<br>necking of Ti |
| 473 K | no bonding | sufficient bonding<br>laminar layers | strong bonding<br>necking of Ti |
| 573 K | no bonding | sufficient bonding<br>laminar layers | sufficient bonding<br>necking of Ti |

A thickness reduction of 30% is not sufficient for roll bonding independent of the working temperature. In contrast, a thickness reduction of 40% is sufficient for bonding, although the bonding strength may be very weak, as in the case of RT deformation. A thickness reduction of 50% yields strong bonding, but also necking of the Ti layers, as shown in Figure 9. Since roll bonding with 40% thickness reduction has been found as most successful, it is used for the following ARB cycles, as well. Further ARB cycles cause deformation localization, as well as the formation of necks, which is found to be independent of temperature. The necks show a random spatial distribution (not shown here).

An increase in rolling temperature facilitates roll bonding of Ti/Al composites at a lower thickness reduction than 50%, which is generally used in ARB processes. At elevated temperatures, Al becomes significantly softer, and therefore, the difference in yield stress between the Al and Ti increases. The deformation becomes unstable and, consequently, results in an increasing number of necks of the Ti layers. By reducing the applied strain, necking can be reduced, but not excluded. Although the second ARB cycle at elevated temperatures has been successful, further processing results in necking of the Ti layers.

### *3.4. Asymmetric ARB*

Asymmetric ARB has been accomplished by means of a four high rolling mill and also with the help of a trio mill. The latter has an asymmetric geometry with respect to the sheet plane, as the working rolls have different diameters, but are operated at the same velocity of the surface. Therefore, the deformation zone is additionally subjected to shear deformation. In order to evaluate the effect of the asymmetric rolling geometry, a sheet obtained from three ARB cycles has been rolled in different rolling mills. Asymmetric rolling has been performed at a trio rolling mill. The diameters of the working rolls were 235 and 290 mm, respectively, and the surface velocity has been set to 3 m/min. The comparative symmetric rolling has been realized utilizing a four high rolling, whose working rolls had a diameter of 110 mm, operated with a surface velocity of 3.5 m/min.

Figure 10 shows the arrangement of the different metallic phases in the cross-section (layer structure) after the fourth ARB cycle with different conditions being applied. It has been found that trio rolling results in a more pronounced necking of the Ti layers.

Thus, at a 50% thickness reduction per cycle, trio rolling is detrimental to achieve continuous lamellar sheets. However, trio rolling enables roll bonding with a 45% thickness reduction, which is not possible by means of a symmetrical four high rolling mill. In order to quantitatively assess the effect of the thickness reduction under asymmetric rolling conditions, a composite was accumulatively roll bonded utilizing a trio mill with a thickness reduction of 50% at each of three cycles with an IHT at 823 K for 90 min being applied after each cycle. In the fourth rolling cycle, the thickness reduction was varied stepwise. Thus, all different deformation states used for further analysis are obtained from one single sheet.

At a reduction of less than 45%, the single sheets do not bond. Between 45% and 50%, the number of necks significantly increases with thickness reduction, as shown in Figure 11. Further thickness reduction does not change the number of necks anymore, but increases the fraction of completely separated layers. However, in comparison to processing with a four high rolling mill, the amount of

separated necks shrinks from 0.4 $mm^{-2}$ to 0.1 $mm^{-2}$. Thus, a low thickness reduction is beneficial for the homogeneity of the deformation process.

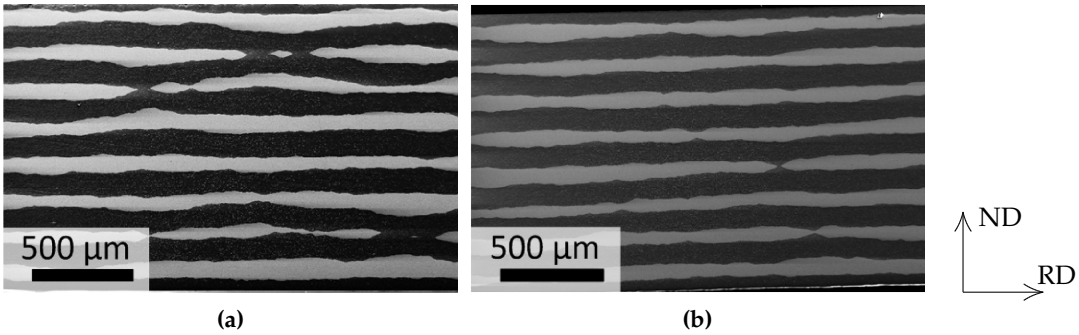


**Figure 10.** Cross-section of the layer structure after four ARB cycles in a trio (**a**) and four high rolling mill (**b**).

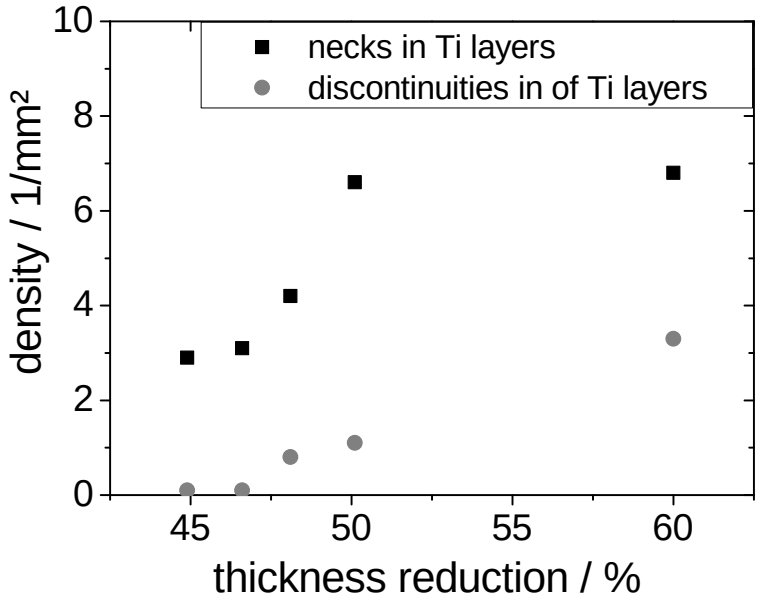


**Figure 11.** Density of necks and separated necks of a Ti/Al composite sheet after four ARB passes in a trio rolling mill in dependence of the thickness reduction during the last rolling cycle.

## 4. Summary

Sheets composed of a high number of alternating Ti and Al layers have been successfully prepared by accumulative roll bonding. In order to keep individual continuous layers, necking occurring predominantly in the Ti layers has to be prevented. This study demonstrated that this is feasible if the applied thickness reduction per rolling step is lowered or if the work hardening rate is increased.

A lower thickness reduction can be achieved by rolling at elevated temperatures and, alternatively, by incorporating a shear component within the deformation zone by utilizing a trio mill. A higher work hardening rate can be achieved by an increased rolling velocity. However, this only works for a high strain rate sensitivity of the Ti layers, which lowers with increasing strength. As a consequence, in order to maintain the low strength and high strain rate sensitivity in the Ti layers, the composites have to be thermally treated after each single ARB cycle. Hence, to obtain materials

with a high specific strength strain, hardening of the composite cannot be achieved while the process demands for continuous layers.

**Acknowledgments:** This work has been supported by the European Union and the Free State of Saxonia in the framework of the European Centre for Emerging Materials and Processes (ECEMP), Contract No. 13795/2379.

**Author Contributions:** Jan Romberg and Jens Freudenberger designed the experiments, collected and interpreted the data, wrote and edited the paper and contributed to all activities. Juliane Scharnweber and Andy Eschke contributed to scanning electron microscopy, including sample preparation, imaging and diffraction; together with Carl-Georg Oertel, they analyzed the results and fostered their interpretation. Hansjörg Bauder, Georg Plattner and Hans Krug performed the accumulative roll bonding experiments; they contributed to the discussion and interpretation of the results and adapted the rolling mill to the present requirements. Frank Holländer performed the hot rolling experiments. Hansjörg Klauß performed the tensile tests. Uta Kühn, Werner Skrotzki, Jürgen Eckert and Ludwig Schultz directed the research and contributed to the discussion and interpretation of the results.

**Conflicts of Interest:** The authors declare no conflict of interest.

## References

1. Kaufmann, H.; Sonsino, C.; Demofonti, G.; Riscifuli, S. High-strength steels in welded state for light-weight constructions under high and variable stress peaks. *Steel Res. Int.* **2008**, *79*, 382–389.
2. Sonsino, C. Light-weight design chances using high-strength steels. *Mater. Und Werkst.* **2007**, *38*, 9–22.
3. Kwon, O.; Lee, K.; Kim, G.; Chin, K. New Trends in Advanced High Strength Steel Developments for Automotive Application. *Mater. Sci. Forum* **2010**, *638–642*, 136–141.
4. Lee, S.; Saito, Y.; Tsuji, N.; Utsunomiya, H.; Sakai, T. Role of shear strain in ultragrain refinement by accumulative roll-bonding ARB process. *Scr. Mater.* **2002**, *46*, 281–285.
5. Shi, M.; Takayama, Y.; Ma, C.; Watanabe, H.; Inoue, H. Microstructure and texture evolution in titanium subjected to friction roll surface processing and subsequent annealing. *Trans. Nonferrous Met. Soc. China* **2012**, *22*, 2616–2627.
6. Belov, N. Sparingly alloyed high-strength aluminum alloys: Principles of optimization of phase composition. *Met. Sci. Heat Treat.* **2012**, *53*, 420–427.
7. Sabirov, I.; Murashkin, M.; Valiev, R. Nanostructured aluminum alloys produced by severe plastic deformation: New horizons in development. *Mater. Sci. Eng. A* **2013**, *560*, 1–24.
8. Valiev, R.; Enikeev, N.; Murashkin, M.; Utyashev, F. Using intensive plastic deformations for manufacturing bulk nanostructure metallic materials. *Mech. Solids* **2012**, *47*, 463–474.
9. Latysh, V.; Semenova, I.; Salimgareeva, G.; Kandarov, I.; Zhu, Y.; Lowe, T.; Valiev, R. *Nanomaterials by Severe Plastic Deformation*; Trans Tech Publications Ltd.: Dürnten, Switzerland, 2006.
10. Sabirov, I.; Perez-Prado, M.; Molina-Aldareguia, J.; Semenova, I.; Salimgareeva, G.; Valiev, R. Anisotropy of mechanical properties in high-strength ultra-fine-grained pure Ti processed via a complex severe plastic deformation route. *Scr. Mater.* **2011**, *64*, 69–72.
11. Bonarski, B.; Mikulowski, B.; Schafler, E.; Holzleithner, C.; Zehetbauer, M. Crystallographic textures of single and polycrystalline pure Mg and Cu subjected to HPT deformation. *Arch. Metall. Mater.* **2008**, *53*, 117–123.
12. Lu, C.; Tieu, K.; Wexler, D. Significant enhancement of bond strength in the accumulative roll bonding process using nano-sized $SiO_2$ particles. *J. Mater. Process. Technol.* **2009**, *209*, 4830–4834.
13. Peng, J.; Liu, Z.; Xia, P.; Lin, M.; Zeng, S. On the interface and mechanical property of Ti/Al-6%Cu-0.5%Mg-0.4%Ag bimetal composite produced by cold-roll bonding and subsequent annealing treatment. *Mater. Lett.* **2012**, *74*, 89–92.
14. Wang, J.; Hoagland, R.; Misra, A. Mechanics of nanoscale metallic multilayers: From atomic-scale to micro-scale. *Scr. Mater.* **2009**, *60*, 1067–1072.
15. Lapovok, R.; Ng, H.; Tomus, D.; Estrin, Y. Bimetallic Copper-Aluminium Tube by Severe Plastic Deformation. *Scr. Mater.* **2012**, *66*, 1081–1084.
16. Marr, T.; Freudenberger, J.; Kauffmann, A.; Romberg, J.; Okulov, I.; Petters, R.; Scharnweber, J.; Eschke, A.; Oertel, C.G.; Kühn, U.; *et al.* Processing of Intermetallic Titanium Aluminide Wires. *Metals* **2013**, *3*, 188–201.

17. Beausir, B.; Scharnweber, J.; Jaschinski, J.; Brokmeier, H.G.; Oertel, C.G.; Skrotzki, W. Plastic anisotropy of ultrafine grained aluminum alloys produced by accumulative roll bonding. *Mater. Sci. Eng. A* **2010**, *527*, 3271–3278.
18. Sauvage, X.; Wilde, G.; Divinski, S.; Horita, Z.; Valiev, R. Grain boundaries in ultrafine grained materials processed by severe plastic deformation and related phenomena. *Mater. Sci. Eng. A* **2012**, *540*, 1–12.
19. Valiev, R.; Islamgaliev, R.; Alexandrov, I. Bulk nanostructured materials from severe plastic deformation. *Prog. Mater. Sci.* **2000**, *45*, 103–189.
20. Zeipper, L.; Zehetbauer, M.; Holzleithner, C. Defect based micromechanical modelling and simulation of nanoSPD CP-Ti in post-deformation. *Mater. Sci. Eng. A* **2005**, *410–411*, 217–221.
21. Pippan, R.; Wetscher, F.; Hafok, M.; Vorhauer, A.; Sabirov, I. The Limits of Refinement by Severe Plastic Deformation. *Adv. Eng. Mater.* **2006**, *8*, 1046–1056.
22. Zehetbauer, M.; Grossinger, R.; Krenn, H.; Krystian, M.; Pippan, R.; Rogl, P.; Waitz, T.; Wurschum, R. Bulk Nanostructured Functional Materials By Severe Plastic Deformation. *Adv. Eng. Mater.* **2010**, *12*, 692–700.
23. Gottstein, G. *Physikalische Grundlagen der Materialkunde*; Springer: Berlin, Germany, 2001
24. Kang, D.H.; Kim, T. Mechanical behavior and microstructural evolution of commercially pure titanium in enhanced multi-pass equal channel angular pressing and cold extrusion. *Mater. Des.* **2010**, *31*, S54–S60.
25. Langdon, T. *Processing of Aluminum Alloys by Severe Plastic Deformation*; Trans Tech Publications Ltd.: Dürnten, Switzerland, 2006.
26. Saito, Y.; Utsunomiya, H.; Tsuji, N.; Sakai, T. Novel ultra-high straining process for bulk material-development of the accumulative roll-bonding (ARB) process. *Acta Mater.* **1999**, *47*, 579–583.
27. Terada, D.; Inoue, S.; Tsuji, N. Microstructure and mechanical properties of commercial purity titanium severely deformed by ARB process. *J. Mater. Sci.* **2007**, *42*, 1673–1681.
28. Saito, Y.; Tsuji, N.; Utsunomiya, H.; Sakai, T.; Hong, R. Ultra-fine grained bulk aluminum produced by accumulative roll-bonding (ARB) process. *Scr. Mater.* **1998**, *39*, 1221–1227.
29. Marr, T.; Freudenberger, J.; Kauffmann, A.; Scharnweber, J.; Oertel, C.G.; Skrotzki, W.; Siegel, U.; Kühn, U.; Eckert, J.; Martin, U.; *et al*. Damascene Light-Weight Metals. *Adv. Eng. Mater.* **2010**, *12*, 1191–1197.
30. Levi, F. Permanent Magnets Obtained by Drawing Compacts of Parallel Iron Wires. *J. Appl. Phys.* **1960**, *31*, 1469–1471.
31. Latypov, M.; Lee, D.; Jeong, H.; Lee, J.; Kim, H. Design of Hierarchical Cellular Metals Using Accumulative Bundle Extrusion. *Metall. Mater. Trans. A* **2013**, *44A*, 4031–4036.
32. Marr, T.; Freudenberger, J.; Seifert, D.; Klauß, H.; Romberg, J.; Okulov, I.; Scharnweber, J.; Eschke, A.; Oertel, C.G.; Skrotzki, W.; *et al.* Ti-Al Composite Wires with High Specific Strength. *Metals* **2011**, *1*, 79–97.
33. Nzoma, E.; Guillet, A.; Pareige, P. Nanostructured Multifilamentary Carbon-Copper Composites: Fabrication, Microstructural Characterization, and Properties. *J. Nan.* **2012**, *2012*, 360818.
34. Dundurs, J. Elastic Interaction of Dislocations with Inhomogeneities. In *Mathematical Theory of Dislocations*; Mura, T., Ed.; ASME: New York, NY, USA, 1969; pp. 70–115.
35. Yang, D.; Hodgson, P.; Wen, C. The kinetics of two-stage formation of $TiAl_3$ in multilayered Ti/Al foils prepared by accumulative roll bonding. *Intermetallics* **2009**, *17*, 727–732.
36. Maier, V.; Höppel, H.; Göken, M. Nanomechanical behavior of Al-Ti layered composites produced by accumulative roll bonding. *J. Phys. Conf. Ser.* **2010**, *240*, 012108.
37. Yang, D.; Cizek, P.; Hodgson, P.; Wen, C. Ultrafine equiaxed-grain Ti/Al composite produced by accumulative roll bonding. *Scr. Mater.* **2010**, *62*, 321–324.
38. Ng, H.; Przybilla, T.; Schmidt, C.; Lapovok, R.; Orlov, D.; Höppel, H.W.; Göken, M. Asymmetric accumulative roll bonding of aluminum-titanium composite sheets. *Mater. Sci. Eng. A* **2013**, *576*, 306–315.
39. Gu, S.; Fang, H.; Zhou, Z.; Du, J. The evolution of microstructure and mechanical properties of Ti/Al composite synthesized by accumulative roll-bonding. *Acta Phys. Sin.* **2012**, *61*, 186104.
40. Hausöl, T.; Maier, V.; Schmidt, C.; Winkler, M.; Höppel, H.; Göken, M. Tailoring Materials Properties by Accumulative Roll Bonding. *Adv. Eng. Mater.* **2010**, *12*, 740–746.
41. Chaudhari, G.; Acoff, V.L. Titanium aluminide sheets made using roll bonding and reaction annealing. *Intermetallics* **2010**, *18*, 472–478.
42. Gurao, N.P.; Sethuraman, S.; Suwas, S. Evolution of Texture and Microstructure in Commercially Pure Titanium with Change in Strain Path During Rolling. *Metall. Mater. Trans. A* **2013**, *44A*, 1497–1507.

43. Romberg, J.; Freudenberger, J.; Scharnweber, J.; Gaitzsch, U.; Marr, T.; Eschke, A.; Kühn, U.; Oertel, C.G.; Okulov, I.; Petters, R.; *et al.* Metallographic Preparation of Aluminium-Titanium Composites. *Pract. Metall.* **2013**, *50*, 739–753.
44. Bouvier, S.; Benmhenni, N.; Tirry, W.; Gregory, F.; Nixon, M.; Cazacu, O.; Rabet, L. Hardening in relation with microstructure evolution of high purity titanium deformed under monotonic and cyclic simple shear loadings at room temperature. *Mater. Sci. Eng. A* **2012**, *535*, 12–21.
45. Chun, Y.; Yu, S.; Semiatin, S.; Hwang, S. Effect of deformation twinning on microstructure and texture evolution during cold rolling of CP-titanium. *Mater. Sci. Eng. A* **2005**, *398*, 209–219.
46. Valiev, R.; Ivanisenko, Y.; Rauch, E. Structure and deformation behavior of armco iron subjected to severe plastic deformation. *Acta Mater.* **1996**, *44*, 4705–4712.
47. Emmens, W. *Formability: A Review of Parameters and Processes that Control, Limit or Enhance the Formability of Sheet Metal*; Springer: Berlin, Germany, 2011; ISBN: 9783642219047.